ELSEVIER

Contents lists available at ScienceDirect

# **Energy Conversion and Management**

journal homepage: www.elsevier.com/locate/enconman



# Thermogravimetric and kinetics investigation of pine wood pyrolysis catalyzed with alkali-treated CaO/ZSM-5



Zhao Sun <sup>a,b</sup>, Bang Xu <sup>b</sup>, Asif Hasan Rony <sup>b</sup>, Sam Toan <sup>b</sup>, Shiyi Chen <sup>a</sup>, Khaled A.M. Gasem <sup>b</sup>, Hertanto Adidharma <sup>b</sup>, Maohong Fan <sup>b,c,\*</sup>, Wenguo Xiang <sup>a,\*</sup>

- a Key Laboratory of Energy Thermal Conversion and Control of Ministry of Education, School of Energy and Environment, Southeast University, Nanjing 210096, China
- <sup>b</sup> Departments of Chemical and Petroleum Engineering, University of Wyoming, Laramie, WY 82071, USA

#### ARTICLE INFO

#### Article history: Received 18 February 2017 Received in revised form 3 April 2017 Accepted 17 April 2017 Available online 21 May 2017

Keywords: Thermogravimetric analysis (TGA) Kinetics Pine wood Pyrolysis CaO/ZSM-5

#### ABSTRACT

In this study, the characteristics of thermal decomposition of Wyoming pine wood catalyzed with CaO/ZSM-5 was investigated by using a thermogravimetric analyzer (TGA). The CaO/ZSM-5 catalyst was prepared using a wet mixing method aided by an ultrasonic treatment to improve the dispersing uniformity of CaO on ZSM-5. Material characterizations such as X-ray diffraction (XRD), X-ray photoelectron spectroscopy (XPS), nitrogen adsorption and desorption isotherms test, and scanning electron microscopy (SEM)/energy dispersive spectrometer (EDS) were carried out to examine thoroughly the CaO/ZSM-5 catalyst. The kinetic parameters and activation energy were determined using the Flynn-Wall-Ozawa (FWO) and Kissinger-Akahire-Sunose (KAS) methods. Results indicate that the yields and conversion of pine wood pyrolysis with CaO/ZSM-5 catalyst addition are much higher than that of pine wood individually. Further, the effect of CaO/ZSM-5 catalyst addition on the activation energy distribution of pine wood pyrolysis is presented and discussed in detail.

 $\ensuremath{\text{@}}$  2017 Elsevier Ltd. All rights reserved.

# 1. Introduction

Fossil fuels are currently one the main sources of energy [1]. However, the burning of fossil fuels releases significant amounts of carbon dioxide into the atmosphere and contributes to the increasing concerns about climate change [2,3]. Biomass is considered to be among the promising alternatives to conventional fuels since it is CO<sub>2</sub> neutral, environmentally friendly and available all over the world [4–7]. Therefore, using biomass as an alternative fuel on a large scale could reduce both the consumption of fossil fuels and the carbon dioxide emission. Moreover, biomass can be converted into more valuable energy carriers using either biochemical or thermo-chemical conversion processes [8-10]. The thermo-chemical conversion technologies can be further divided into combustion, pyrolysis, gasification process, and so forth. Pyrolysis is thermal decomposition of biomass occurring in the absence of oxygen and relatively low temperature, which is generally the first step in combustion and gasification processes.

coke tolerance and good stability in recycling.

In comparison, CaO can be used as the catalyst for cracking heavy compounds into light oxygenated compounds, which can be converted into aromatics over HZSM-5 catalyst [24–26]. Studies also indicate that the CaO catalyst could convert the acids into hydrocarbons by the decarboxylation reactions [27]. Thus, CaO is seen to be an effective catalyst for the upgrading of bio-oils and

Among the various ways of biomass utilization, catalytic pyrolysis has attracted particular attention in recent years [11–14]. The catalytic pyrolysis process is seen as a potential application for environmentally friendly conversion of biomass into valuable products. In this regard, the ZSM-5 zeolite is seen to be an efficient catalyst for degradation of biomass due to its strong acidity and unique pore structure [15,16]. Currently, several approaches have been used to obtain the hierarchical ZSM-5 zeolite which has been proven to enhance the diffusion ability and catalytic performance [17-20]. The desilication method by alkali treatment is proved to be a novel, effective and simple strategy for creating mesopores over ZSM-5 zeolite [21]. Groen et al. [22] have directly demonstrated the enhanced diffusion ability of the alkali-treated ZSM-5 zeolite. HZSM-5 zeolite has also been tuned into highly active by generating hierarchical pores via alkali treatment, which removes the amorphous phase and produces mesopores connecting microchannel [23]. The hierarchical porous zeolite shows excellent

<sup>&</sup>lt;sup>c</sup> School of Energy Resource, University of Wyoming, Laramie, WY 82071, USA

<sup>\*</sup> Corresponding authors at: Departments of Chemical and Petroleum Engineering, University of Wyoming, Laramie, WY 82071, USA (M. Fan); Key Laboratory of Energy Thermal Conversion and Control of Ministry of Education, School of Energy and Environment, Southeast University, Nanjing 210096, China (W. Xiang).

E-mail address: mfan@uwyo.edu (M. Fan).

enhancing biomass conversion. However, CaO can be deactivated easily during the pyrolysis process [28]. Lu et al. [24] explored fast pyrolysis of biomass over Py-GC/MS and demonstrated that the addition of CaO could reduce the levels of phenols and eliminated the acids, and it could increase the formation of cyclopentanones, hydrocarbons, and several light compounds. Therefore, in order to design a novel catalyst and prevent CaO deactivation, the alkali-treated ZSM-5 catalyst is used to provide sufficient surface area for biomass pyrolysis and improve the quality of generated bio-oil.

A good understanding of the decomposition of biomass during thermochemical conversion is important for developing efficient processing technology. Thus, it is important to investigate the kinetics characterization of biomass utilization. The investigation of pyrolysis kinetics of biomass and catalytic pyrolysis have been widely studied by many researchers [29–34,26]. However, a very limited investigation could be found for the influence of ZSM-5 and CaO blends on the pyrolytic behavior of biomass. In thermal and kinetic analyses of biomass pyrolysis, thermogravimetric analysis (TGA) is one of the most commonly applied thermo-analytical technique. TGA measures the weight loss caused by the release of volatiles during thermal decomposition as a function of time [35]. To model pyrolysis using TGA data, iso-conversional and model-fitting are the two main methods for determining the kinetic parameters and the reaction mechanism [36,37].

The focus herein is to investigate the characteristics and kinetics of the pine wood pyrolysis. Thermal behavior of pine wood pyrolysis using CaO and CaO/ZSM-5 catalysts with different Ca/C ratios (0, 0.1, 0.2, and 0.3) and different heating rates (10 °C/min, 20 °C/min, 30 °C/min, and 40 °C/min) were determined by TGA, respectively. In this study, the iso-conversional method is adopted due to its simplicity and accuracy in estimating the activation energy (E) independent of the reaction mechanism [38,39]. Specifically, Flynn-Wall-Ozawa (FWO) and Kissinger-Akahira-Sunose (KAS) methods are applied for E determination [40].

The specific objectives of this study are to:

- (1) Investigate the pine wood pyrolysis mechanism over modified CaO/ZSM-5 catalyst.
- (2) Explore the decomposition behavior at different heating rate and Ca/C ratios.
- (3) Enhance the biomass conversion and syngas and bio-oil production during pyrolysis process.
- (4) Estimate the activation energy distributions and prepare for designing biomass pyrolysis reactor system.

# 2. Material and methods

# 2.1. Samples and catalysts preparation

In this experiment, pine wood biomass obtained from the State of Wyoming in the US is used for thermogravimetric analysis. The pine wood was treated through a procedure comprised of drying, crushing, milling, and sieving to achieve a particle size below 0.15 mm. After drying at 105 °C for 24 h, the proximate, and ultimate analysis were performed twice, and the results are presented in Table 1. The proximate analysis was carried out according to the Chinese standard procedure GB/T 212-2001. The elemental analysis was determined by an elemental analyzer. Comparisons of the functional groups of the biomass pyrolysis at different temperatures were also determined using FTIR analyses in the region of 500–4000 cm<sup>-1</sup>, as depicted in Fig. 1.

Commercial NH<sub>4</sub>-ZSM-5 zeolite (SiO<sub>2</sub>/Al<sub>2</sub>O<sub>3</sub> = 80) and nano-CaO (Sigma-Aldrich) were used as the precursors for nano-CaO-ZSM-5 catalyst preparation. The detailed preparation method is as follows: 5 g of ZSM-5 zeolite were added to 100 mL of distilled water

**Table 1**Proximate and ultimate analysis of the pine wood.

Proximate analysis (% by weight)	
Fixed carbon	16.50
Volatile	78.12
Moisture	5.09
Ash	0.29
Ultimate analysis (% by weight)	
Carbon	50.36
Hydrogen	6.20
Nitrogen	0.33
Oxygen	43.06
Sulfur	0.05

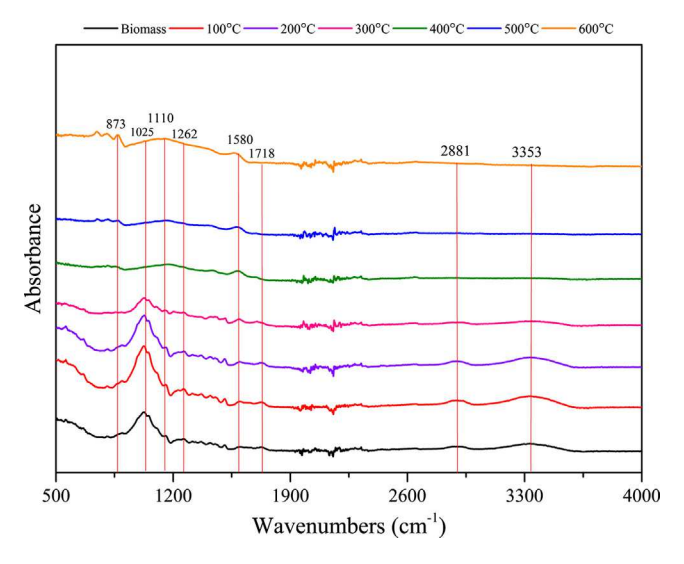


Fig. 1. FTIR spectra of pinewood at different pyrolysis temperature under  $N_2$  atmosphere.

to form the suspension. Then, 5 g of nano-CaO were added into the suspension gradually while stirring simultaneously. The resultant suspension was treated by ultrasound for 30 min. Finally, the mixture was dried at 80 °C for 12 h and calcined at 600 °C for 3 h. The preparations of CaO-zeolite catalyst using a wet mixing method can be seen in previous works [41,42].

# 2.2. Catalyst characterization

Scanning electron microscope (SEM) and energy dispersive spectrometer (EDS) were used to determine the textural, structure, and chemical performances of the ZSM-5 zeolite, CaO, and alkalitreated CaO/ZSM-5 catalysts. The crystal structure of the catalysts was measured by X-ray diffraction (XRD) analysis, which was conducted by a Rigaku Smartlab diffractometer with a Cu K $\alpha$  radiation source. X-ray photoelectron spectroscopy (XPS) analysis was carried out to provide an additional examination of the CaO/ZSM-5 catalyst surface composition. Details on the operational parameters are given in our previous studies [43]. Temperatureprogrammed desorption (TPD) was conducted in a quartz reactor equipped with an online mass spectrometer (Hiden, HPR-20 QIC), where 0.1 g of the samples was used for each run. The catalyst was pre-outgassed by the helium at 150 °C for 30 min. When the catalyst was cooled down to 30 °C, a flow of CO2-helium gas mixture was fed through the catalyst for 1 h of CO2 adsorption at 30 °C. The residual CO<sub>2</sub> was kept under the helium environment for 1 h. Then, the CO<sub>2</sub>-TPD experiment was carried out from 30 °C to 850 °C at a heating rate of 10 °C/min under the atmosphere of helium.

#### 2.3. Thermogravimetric analysis

The thermogravimetric experiments were completed using the SDT Q600 thermogravimetric analyzer. In this study, pine wood and catalysts are mixed by using mechanical a mixing method according to different Ca/C ratios. The mixture of pine wood and catalyst was then grounded to obtain the uniform pine woodcatalyst samples. All the samples (5-10 mg) were heated from room temperature to 1000 °C and kept in the nitrogen atmosphere for 10 min. Then, an excess of oxygen was fed into the furnace at a flow rate of 5 mL/min to burn the solid residue. The N2 flow rate was set to 60 mL/min through all the experimental conditions (10 °C/min, 20 °C/min, 30 °C/min and 40 °C/min, respectively). For each Ca/C ratio and heating rate, three repetitive TG curves were obtained in order to assure reproducibility of the results. We estimate that the uncertainty in the final conversion of pine wood pyrolysis at each condition no to exceed 1%. The Ca/C ratio is defined as the molar mass of CaO in the catalyst, divided by molar mass of carbon in pine wood, as shown below:

$$Ca/C$$
 ratio =  $\frac{Molar\ mass\ of\ CaO\ in\ catalyst}{Molar\ mass\ of\ carbon\ in\ pine\ wood}$ 

The biomass conversion is calculated as:

$$\textit{Biomass conversion} = \frac{m_t - m_f - m_c}{m_i - m_f - m_c} \times 100\%$$

where  $m_i$  is the initial mass of the sample,  $m_t$  refers to the mass of the sample at time t,  $m_f$  denotes the final residue mass of the sample, and mc refers to the final mass of catalyst.

# 2.4. Kinetic model

In a linear non-isothermal thermo-gravimetric analysis (TGA), the sample was heated at a constant heating rate ( $\beta$  = dT/dt). The weight loss of the sample with temperature changes is noted and used for TG and DTG analyses. Generally, the reaction rate d $\alpha$ /dT is expressed by the decomposition rate given in Eq. (1):

$$\frac{d\alpha}{dt} = k(T)f(\alpha) \tag{1}$$

where  $f(\alpha)$  represents the temperature-independent conversion function. T is the absolute temperature (K), k is the reaction constant, and  $\alpha$  represents the conversion, which is defined:

$$\alpha = \frac{m_i - m_t}{m_i - m_f} \tag{2}$$

where  $m_i$ ,  $m_t$ , and  $m_f$  refer to the initial mass of the sample, the mass of the sample at time t, and the final mass of the sample in the reaction. k(T) can be described by the Arrhenius equation as:

$$k = A \exp\left(-\frac{E}{RT}\right) \tag{3}$$

where A (1/s) is the apparent pre-exponential factor, E (J/mol) represents the activation energy, and R (J·mol $^{-1}$ ·K $^{-1}$ ) represents the ideal gas constant;

The combination of Eqs. (1) and (3) gives:

$$\frac{d\alpha}{dt} = A \exp\left(-\frac{E}{RT}\right) f(\alpha) \tag{4}$$

when the heating rate  $\beta$  (K/min):

$$\beta = \frac{dT}{dt} \tag{5}$$

is introduced, Eq. (4) can be transformed into:

$$\frac{d\alpha}{dT} = \frac{A}{\beta} \exp\left(-\frac{E}{RT}\right) f(\alpha) \tag{6}$$

which describes the time evolution of physical and chemical changing within the decomposition process. The integrated form of Eq. (6) is generally expressed as:

$$G(\alpha) = \int_0^\alpha \frac{d\alpha}{f(\alpha)} = \frac{A}{\beta} \int_{T_0}^T \exp\left(-\frac{E}{RT}\right) dT$$
 (7)

$$T = T_0 + \beta t \tag{8}$$

where  $G(\alpha)$  is the integrated form of conversion-dependent function  $f(\alpha)$ , and  $T_0(k)$  is the starting temperature.

Due to their simplicity and reliability, the Flynn-Wall-Ozawa (FWO) and Kissinger-Akahire-Sunose (KAS) iso-conversional methods were used to calculate the activation energy [38]. The Flynn-Wall-Ozawa (FWO) equation can be written as:

$$\ln \beta = \ln \left( \frac{0.0048 A E_{\alpha}}{Rg(\alpha)} \right) - 1.0516 \frac{E_{\alpha}}{RT}$$
 (9)

where  $\alpha$  is equal to a constant. The values of  $ln\beta$  and 1/T are correlated by a straight line, and the activation energy is calculated by its slope. Thus, a series of activation energies can be obtained corresponding to different  $\alpha$  values. Similarly, the KAS equation is expressed as:

$$\ln\left(\frac{\beta}{T_{\alpha}^{2}}\right) = \ln\left(\frac{AR}{E_{\alpha}g(\alpha)}\right) - \frac{E_{\alpha}}{RT_{\alpha}} \tag{10}$$

The activation energy can also be determined from a plotting  $\ln\left(\frac{\beta}{T_{-}^2}\right)$  vs. 1/T.

## 3. Results and discussion

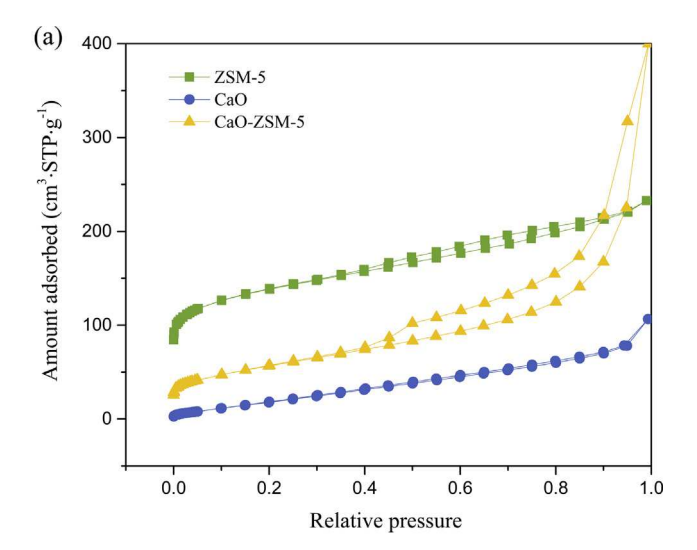
# 3.1. Characterization of pine wood and fresh catalysts

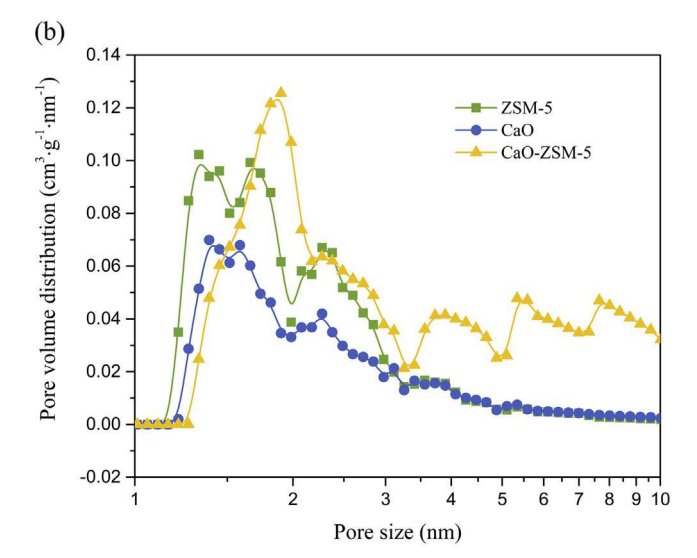
# 3.1.1. FTIR analysis of pine wood

The functional groups of pyrolysis pine wood under different temperatures (from 100 °C to 600 °C) were determined using FTIR spectra in the region 500–4000 cm<sup>-1</sup> and the output is presented in Fig. 1. The assignment of absorption bands for the pine wood can be obtained according to the characteristic infrared absorption frequencies [44]. Differences in the spectra with N<sub>2</sub> pyrolysis at different temperature were mainly observed in the FTIR spectra. The intensity of the -OH bands around 3350 cm<sup>-1</sup> decreased with temperature increase and disappeared after 400 °C. It can also be seen that several bands show the same tendency with —OH bands, which were assigned to the C—H stretching vibration (2881 cm<sup>-1</sup>), aliphatic C=O and -COOH stretching vibrations (1718 cm<sup>-1</sup>), aromatic C=C stretching modes (1262 cm<sup>-1</sup>), and C-O stretching (1025 cm<sup>-1</sup>), respectively [45,46]. A low absorbance peak observed in the region 1110 cm<sup>-1</sup> was assigned to the C—C bond, and the peak becomes wider with increasing temperature. The peaks presented in the region 1500-1680 cm<sup>-1</sup> were attributed to the aromatic C=C stretching modes, and the peaks become slightly stronger with increasing temperature. In addition, a small peak due to the -CH2 out-of-plane bending vibration was found at the wavenumber of 873 cm<sup>-1</sup>. The results are in agreement with previous work on the effect of temperature on biomass pyrolysis [47].

# 3.1.2. $N_2$ adsorption and desorption analysis

The sorption isotherms of ZSM-5 zeolite, CaO, and CaO/ZSM-5 samples are shown in Fig. 2(a). It can be seen that the amount of  $N_2$  adsorbed on the CaO/ZSM-5 catalyst is intermediate to that observed for ZSM-5 zeolite and CaO. Further, at a relative pressure  $P/P_0$  greater than 0.8, a sharp increase in adsorption is observed for this catalyst. The high adsorption of  $N_2$  at the relatively low-pressure area indicates the significant presence of micropores for





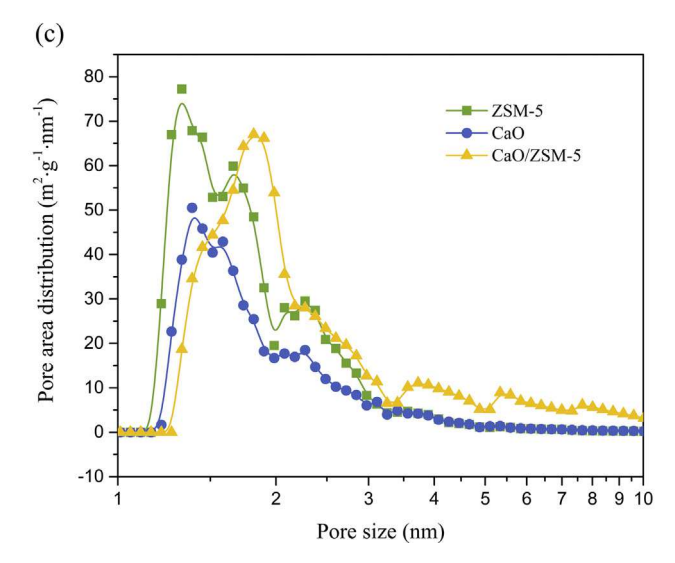


**Fig. 2.** Porosity characteristics of ZSM-5 zeolite, nano-CaO, and CaO/ZSM-5 [a:  $N_2$  adsorption-desorption isotherms; b: Pore volume distribution; c: pore area distribution].

the ZSM-5 zeolite and CaO/ZSM-5 catalyst. The phenomenon of adsorption hysteresis illustrates the existence of mesopores, especially for the alkali-treated CaO/ZSM-5 catalyst. As shown in

**Table 2**Ash composition of pine wood samples by using XRF analysis.

Compound	Biomass ash (%)
SiO <sub>2</sub>	6.45
$Al_2O_3$	1.93
$Fe_2O_3$	2.54
CaO	42.90
MgO	13.61
Na <sub>2</sub> O	1.05
K <sub>2</sub> O	14.76
$MnO_2$	3.58
$P_{2}O_{5}$	2.69
SrO	0.24
BaO	0.18
SO <sub>3</sub>	1.63

Table 2, the BET surface areas of these three samples are  $413.5 \, \text{m}^2/\text{g}$ ,  $87.3 \, \text{m}^2/\text{g}$ , and  $204.0 \, \text{m}^2/\text{g}$ , respectively. The pore volume distributions and pore area distributions of ZSM-5 zeolite, CaO, and CaO/ZSM-5 catalysts are presented in Fig. 2(b) and Fig. 2(c), respectively. Fig. 2(b) shows that the pore volume of the alkali-treated CaO/ZSM-5 catalyst is distributed uniformly from pore size 2–10 nm. Further, Fig. 2(b) and (c) show that the pore volume and pore area of the modified CaO/ZSM-5 catalyst are much higher than that of ZSM-5 zeolite and Ca for pore sizes less than 2 nm and slightly higher when the pore size is greater than 2 nm. These results indicate that the hierarchical mesoporous structure could promote the gas diffusion ability and catalytic performance [19]. Thus, the modified catalyst was seen to significantly contribute to CO<sub>2</sub> capture, oil selectivity, and biomass conversion.

# 3.1.3. XRD analysis

XRD patterns of ZSM-5 zeolite, CaO, and CaO/ZSM-5 are presented in Fig. 3. As shown, the CaO and ZSM-5 samples produce specific peaks and their crystals are characterized to be calcium oxide (1467) and zeolite ZSM-5 (003), respectively. For CaO/ZSM-5 catalyst, two small peaks are detected at approximately 23° and 29°, which is inferred to be a mixture of sodium oxide, calcium oxide, and silicon oxide (138). This information indicates that the CaO is dispersed uniformly in the skeleton structure of the alkali-treated ZSM-5 zeolite. Further, XPS and SEM/EDS analyses

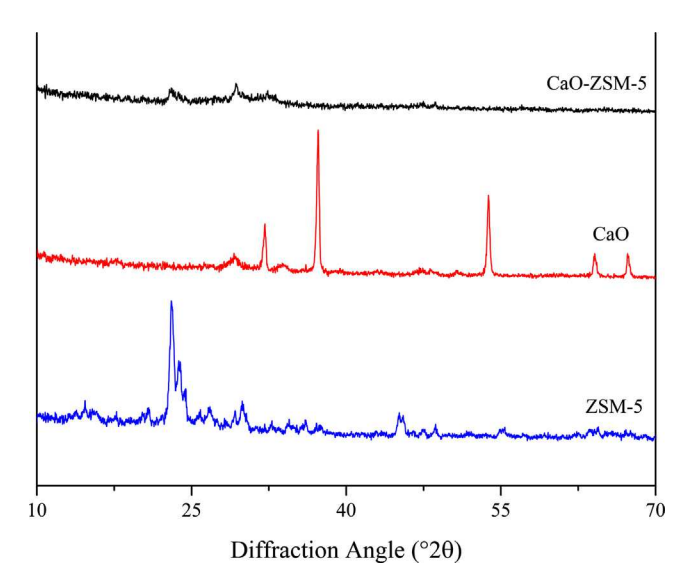
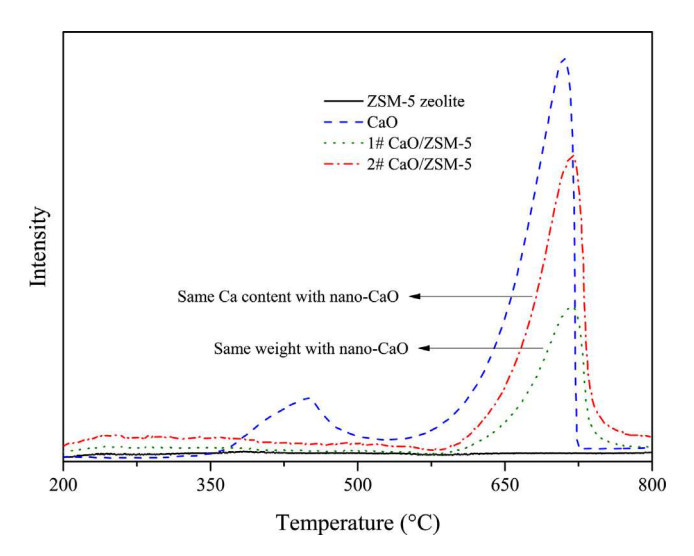


Fig. 3. XRD patterns of ZSM-5 zeolite, CaO, and the alkali-treated CaO/ZSM-5 catalyst.



**Fig. 4.** XPS spectra of fresh CaO/ZSM-5 catalyst [a: Large scale XPS spectra from 0 to 800 eV; b: high resolution XPS spectra of the Ca 2p peaks; c: high-resolution XPS spectra of the C 1s peaks; and d: high resolution XPS spectra of the Si 2p peaks].

are carried out to verify the assumption and further investigate the catalyst composition and elemental distributions.

# 3.1.4. TPD analysis

The CO<sub>2</sub>-TPD analysis is used to investigate the alkalinity characteristics of the ZSM-5 zeolite, CaO, and CaO/ZSM-5, as shown in

Fig. 4. In order to compare the peak intensity more clearly, two CO<sub>2</sub>-TPD experiments (1# and 2#) were carried out for the CaO/ ZSM-5 catalyst, which indicates the same weight addition with CaO catalyst and same CaO content addition with CaO catalyst respectively. It can be seen that the ZSM-5 zeolite shows minimal response to the temperature programmed desorption experiment. CaO shows two CO<sub>2</sub> desorption peaks at 440-450 °C and 700-710 °C, respectively. After incorporating the alkali-treated ZSM-5 zeolite with CaO, the peak at 440-450 °C disappears as seen in 1# CaO/ZSM-5 and 2# CaO/ZSM-5, which represent the same weight and same calcium content with CaO, respectively. Moreover, the strong desorption peak (700-710 °C) shifts slightly at a high-temperature range (710-720 °C), and the intensity of #2 CaO/ZSM-5 catalyst decreases slightly compared with CaO. During the calcination process at 600 °C, the NH<sub>4</sub>-ZSM-5 is converted into HZSM-5 and promotes the acidity of the ZSM-5 zeolite. Thus, the addition of HZSM-5 zeolite decreases the amount of CO<sub>2</sub> desorption of the CaO/ZSM-5 catalyst to some extent and improves the CO<sub>2</sub> desorption temperature. The results also explain the thermogravimetric analysis results as shown below.

## 3.1.5. XPS analysis

To confirm the expected compositions of the modified CaO/ZSM-5 samples, all peaks (O 1s, Ca 2p, C 1s, and Si 2p) relevant to this study are identified, as shown in Fig. 5. Most importantly, XPS analysis was carried out to obtain data on the relative intensities of the detected peaks, thus assisting in determining the elemental distributions at the surface of the catalyst. The full-range XPS spectra results seen in Fig. 5(a) qualitatively

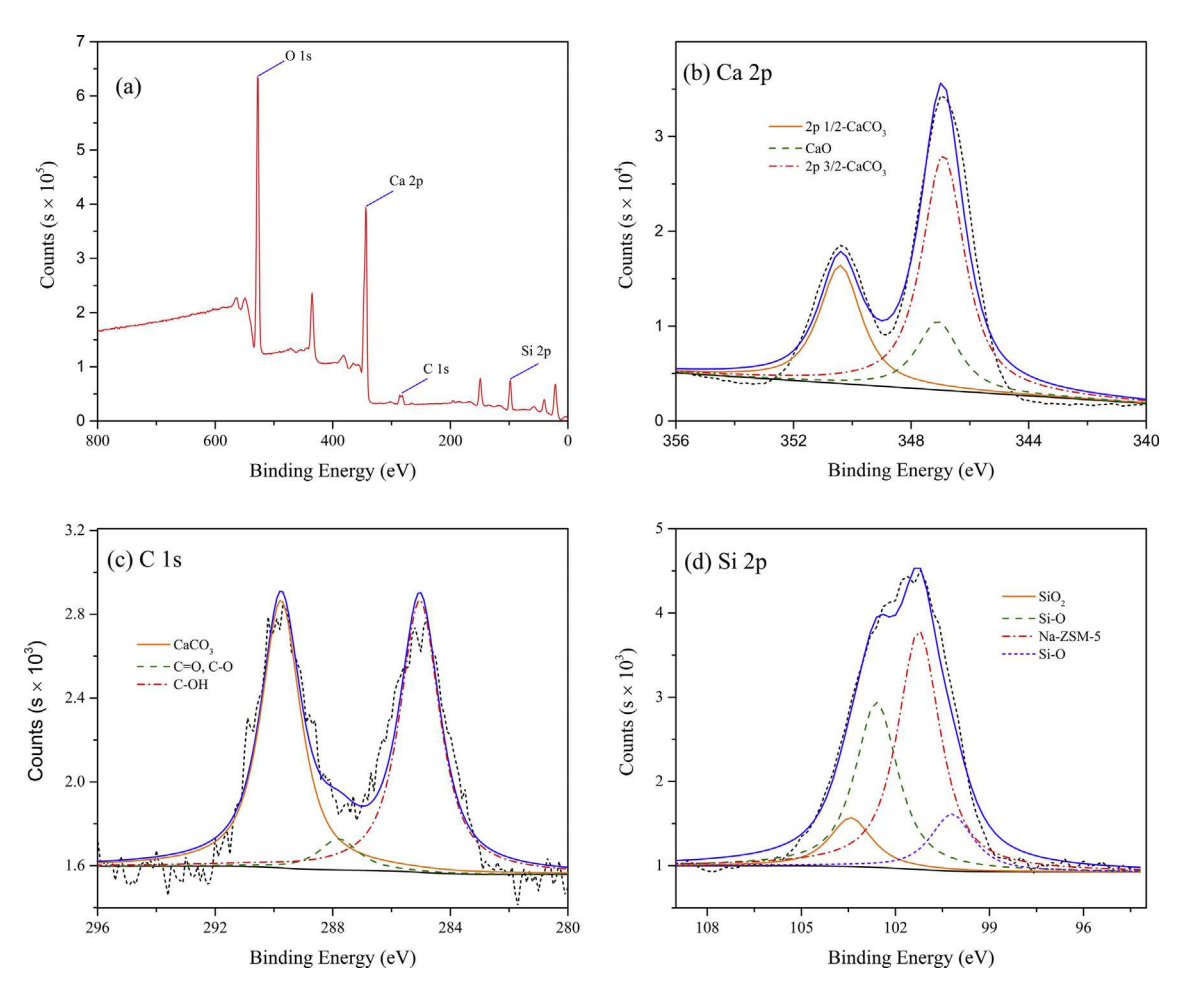


Fig. 5. SEM images and EDS mapping (calcium, silica, alumina, and sodium distributions, respectively) for the alkali-modified CaO/ZSM-5 catalyst.

revealed the existence of Si, Ca, O, and C elements with atomic percent accounts for 15.3%, 20.2%, 57.2%, and 7.0%, respectively, on the surface of the modified samples. High-resolution XPS spectra of Ca 2p, C 1s, and Si 2p were analyzed to determine the chemical environment of the alkali-treated CaO/ZSM-5 catalyst. As shown in Fig. 5(b), two major peaks located at 346.9 eV and 350.4 eV appeared to result from the CaCO3 spin-orbit doublet (CaCO<sub>3</sub> 2p <sub>1/2</sub> and CaCO<sub>3</sub> 2p <sub>3/2</sub>, respectively) with a splitting of 3.5 eV. Another Ca 2p peak appeared at 347.1 eV approximately which could be attributed to chemical bonding of calcium and oxide [48]. As for C 1s spectra seen in Fig. 5(c), the spectra was fitted with a sum of three components: C-OR (285.4 eV), carbon-oxygen single bond and carbon-oxygen double bond C-O, C=O (287.8 eV), and carbonate CaCO<sub>3</sub> (289.4 eV). Thus, it can be concluded that the surface of the catalyst is composed of CaO, CaCO<sub>3</sub>, and Ca(HCO<sub>3</sub>)<sub>2</sub> As such, the CaO reacts with the carbon dioxide and moisture in the air to form a small amount of CaCO3 and Ca(HCO3)2 at the catalyst surface. Fig. 5(d) shows that the peak of Si 2p XPS spectra is quite broad and appears to consist of three bonding environments, which are Si-O (100.2 and 102.6 eV), SiO<sub>2</sub> (103.5 eV), and Na-ZSM-5 (101.2 eV), respectively.

#### 3.1.6. SEM and EDS analysis

Fig. 6 presents the particle shape and distributions of CaO/ZSM-5 catalyst. As shown, the particles of the modified CaO/ZSM-5 are fine and highly dispersed, which verify the XRD and BET results. The modified CaO/ZSM-5 shows a hierarchical pore structure which is expected to enhance the diffusion ability and catalytic performance. In addition, the particles brightness is different due to the different amount of carbon deposition during SEM samples preparation process. EDS analysis is used to further investigate the elemental composition at different brightness regions and determine the elemental distributions for Ca, Si, Al, and Na. The EDS results indicate that varied carbon content leads to the different brightness. The EDS mapping is also carried out to analyze the Ca, Si, Al, and Na elements distributions. Here, the brighter the region, the higher content it represents. The mapping shows that silicon and calcium produce comparable distributions, which indicates that the calcium is dispersed and surrounds the skeleton structure of the alkali-treated ZSM-5 zeolite. In comparison, the contents of sodium and alumina are relatively low. The EDS mapping results show that the CaO was attached to the framework or dispersed in the hieratical pore structure of the alkali-treated ZSM-5 zeolite uniformly.

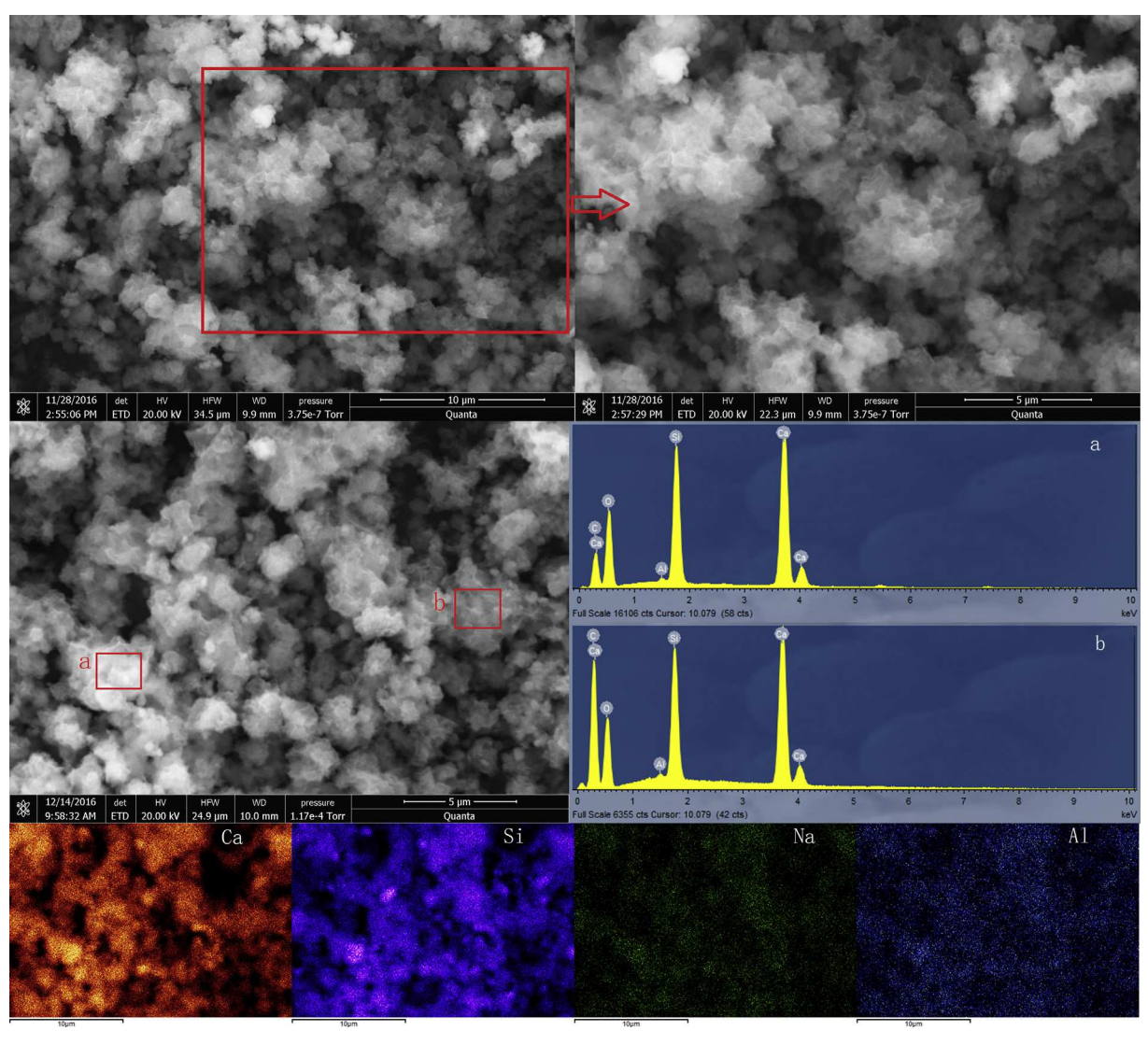


Fig. 6. The CO<sub>2</sub>-TPD profiles of ZSM-5 zeolite, CaO, and CaO/ZSM-5 catalysts.

## 3.2. Thermogravimetric analysis

# 3.2.1. Effect of the heating rate

Thermal behavior of pine wood with catalysts (CaO and CaO/ZSM-5) blends was determined using SDT Q600 thermogravimetric analyzer (TGA). The TG and DTG curves of (a) pine wood, (b) pine wood with CaO blends, (c) and pine wood with CaO/ZSM-5 blends at Ca/C ratio of 0.2 at the heating rates of 10 °C/min, 20 °C/min, 30 °C/min, and 40 °C/min are presented in Fig. 7. In Fig. 7(a), the heating rate shows significant effects on the DTG curves but the biomass conversions after 500 °C remained basically the same with

increasing heating rate. Both TG and DTG curves reveal that the pine wood pyrolysis process occurs mainly in three stages (dehydration, volatilization, and decomposition). The first stage, from room temperature to 250 °C, corresponded to a loss of moisture and the very light volatile materials. Most of the weight loss is occurred in the second stage from 250 to 400 °C approximately. The weight loss of the second stage (250–400 °C) is attributed to the decomposition of hemicellulose and cellulose, while the third stage (400–700 °C) is due to the slow decomposition of lignin [49]. Some non-volatile carbon compounds also vaporize and form CO and CO<sub>2</sub> in the third stage due to the high temperatures [38].

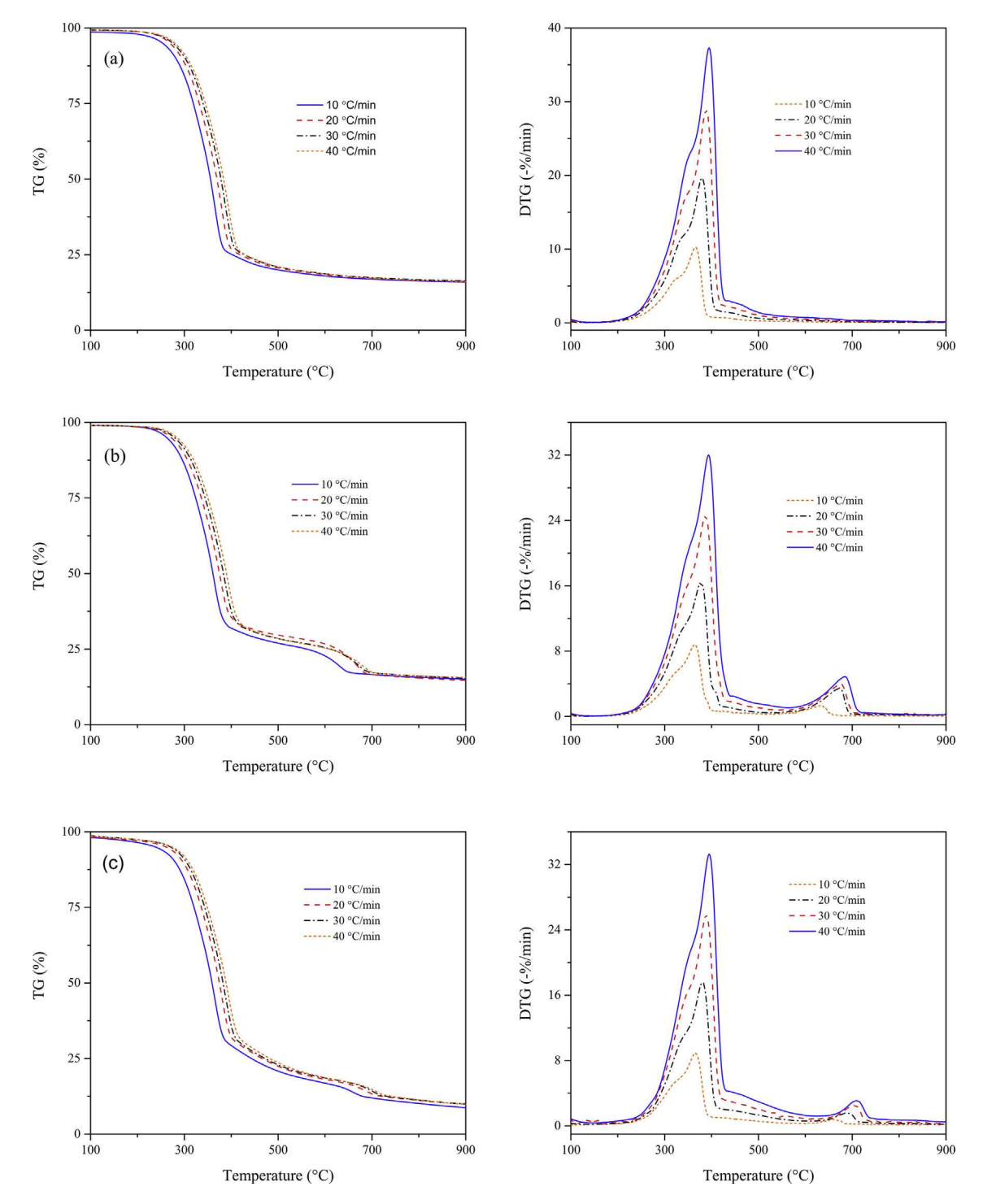


Fig. 7. TG and DTG curves of biomass pyrolysis at different heating rate (10 °C/min, 20 °C/min, 30 °C/min and 40 °C/min) under the Ca/C ratio = 0.2 [a: TG and DTG curves of pine wood; b: TG and DTG curves of pine wood with CaO/ZSM-5 catalyst blends].

The TG and DTG curves of catalytic pyrolysis using CaO catalysts are different from that of pine wood pyrolysis without catalyst addition. Two more stages are observed due to the existence of CaO during the pine wood pyrolysis process, as presented in Fig. 7(b). It can be concluded from the DTG curve that the decomposition of cellulose and hemicellulose occurs mainly at temperatures lower than  $400\,^{\circ}$ C. During the second stage, calcium oxide absorbs the released  $CO_2$  so that the mass reduction is delayed compare with the pure pine wood pyrolysis experiment. The fourth stage occurred when the temperature is higher than  $650\,^{\circ}$ C.  $CaCO_3$  decomposes to be CaO and  $CO_2$ , thus a rapid weight decrease and smalls peak were found at the fourth stage. The generated  $CO_2$  will also react with biochar at a relatively high temperature and thus improve the biomass conversion.

For the catalytic pyrolysis process with CaO/ZSM-5 catalyst blends, the TG and DTG curves show a similar tendency for the first two stage as seen in Fig. 7(c). Compared with co-pyrolysis of pine wood and CaO, the weight loss rate increases a lot for the third stage. It has been proved that ZSM-5 can markedly enhance the deoxygenation reaction during lignin pyrolysis, reducing the oxygen content of the lignin produced bio-oil [50]. Thus, it can be concluded that the addition of alkali-treated CaO/ZSM-5 catalyst could

promote the deoxygenation. A higher lignin conversion could be obtained with CO or CO<sub>2</sub> gas generation by using CaO/ZSM-5 catalyst during the third pyrolysis stage. Further, the released steam from Ca(OH)<sub>2</sub> also enhance the pine wood conversion to some extent. The CaCO<sub>3</sub> decomposition reaction occurs at the fourth stage which leads to a DTG peak seen in Fig. 7(c). For the fifth stage, the weight loss of the pine wood sample with CaO/ZSM-5 catalyst blends is still higher compared with the weight loss of pure pine wood and CaO blended. The gradually released CO<sub>2</sub> gas further promotes the pine wood conversion at a relatively high temperature. The pyrolysis mechanism with applied CaO/ZSM-5 catalyst is shown in the Graphical Abstract and the main reaction during the whole biomass pyrolysis using CaO catalyst is summarized as shown below:

Biomass pyrolysis: Biomass

$$\rightarrow Gases(H_2+CO+CO_2+H_2O+CH_4+CnHm)+Tar+Char \eqno(11)$$

$$CaO \ absorption: CaO + CO_2 \rightarrow CaCO_3 \eqno(12)$$

CaO hydration: 
$$CaO + H_2O \rightarrow Ca(OH)_2$$
 (13)

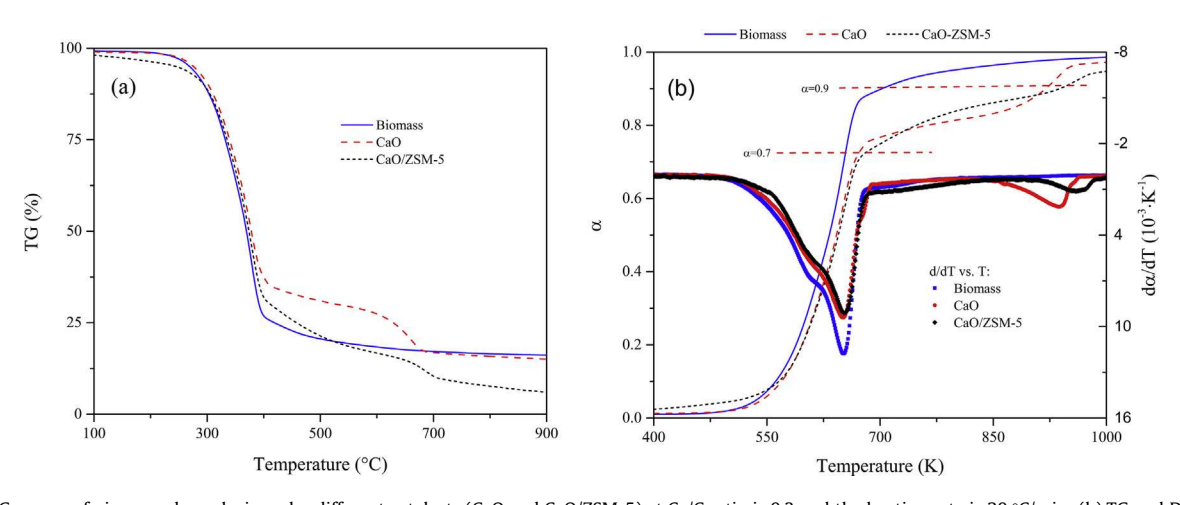


Fig. 8. (a) TG curves of pine wood pyrolysis under different catalysts (CaO and CaO/ZSM-5) at Ca/C ratio is 0.3 and the heating rate is 20 °C/min; (b) TG and DTG profiles in forms of temperature,  $\alpha$  and temperature, d $\alpha$ .

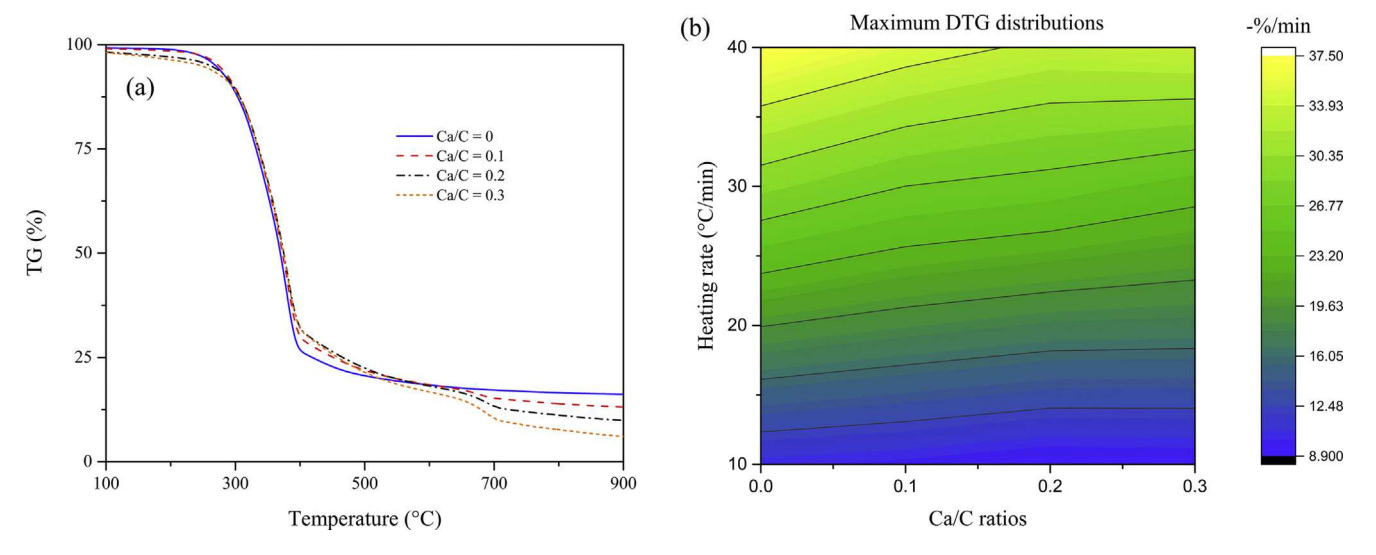


Fig. 9. Effect of Ca/C ratios and heating rates on pine wood pyrolysis under the heating rate is 20 °C/min (a) TG curves of pinewood pyrolysis at different Ca/C ratios (0, 0.1, 0.2, and 0.3); (b) The maximum DTG distributions during pine wood pyrolysis process.

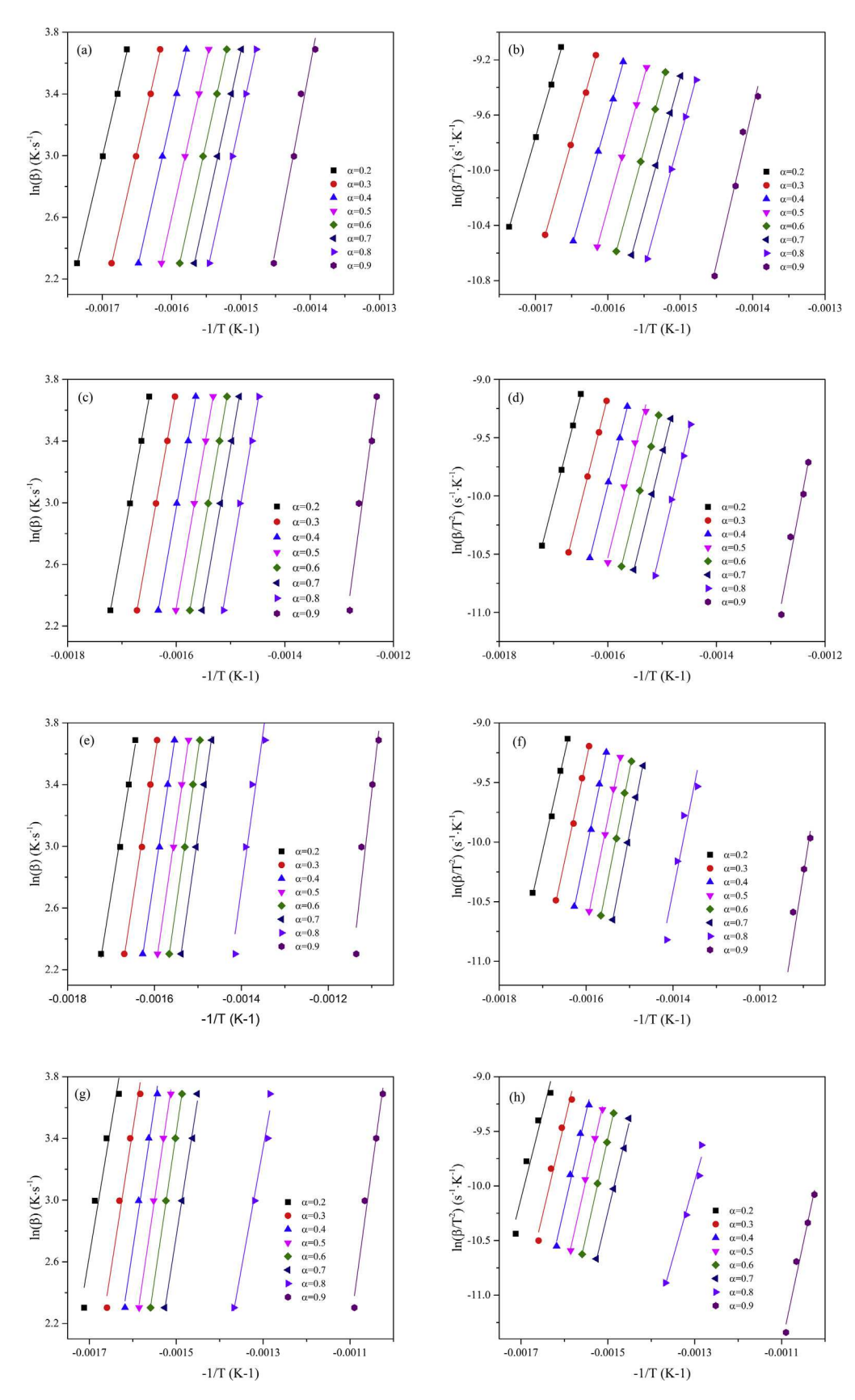


Fig. 10. Plots for determination of activation energy under the conversions from 0.2 to 0.9: (a) plots of  $\ln(\beta)$  versus  $-1/\Gamma$  of pinewood; (b) plots of  $\ln(\beta/\Gamma^2)$  versus  $-1/\Gamma$  of pinewood; (c)  $\ln(\beta)$  versus  $-1/\Gamma$  of CaO/ZSM-5, Ca/C = 0.1; (d)  $\ln(\beta/\Gamma^2)$  versus  $-1/\Gamma$  of CaO/ZSM-5 Ca/C = 0.1; (e)  $\ln(\beta)$  versus  $-1/\Gamma$  of CaO/ZSM-5, Ca/C = 0.2; (f)  $\ln(\beta/\Gamma^2)$  versus  $-1/\Gamma$  of CaO/ZSM-5, Ca/C = 0.2; (g)  $\ln(\beta)$  versus  $-1/\Gamma$  of CaO/ZSM-5, Ca/C = 0.3 (h)  $\ln(\beta/\Gamma^2)$  versus  $-1/\Gamma$  of CaO/ZSM-5, Ca/C = 0.3.

$$Ca(OH)_2$$
 dehydration :  $Ca(OH)_2 \rightarrow CaO + H_2O$  (14)

$$CaCO_3$$
 decomposition :  $CaCO_3 \rightarrow CaO + CO_2$  (15)

Biochar oxidation : 
$$CO_2 + C \rightarrow 2CO$$
  $H_2O + C \rightarrow CO + H_2$  (16)

# 3.2.2. Effect of catalysts addition

Fig. 8 presents the effect of catalysts (CaO and CaO/ZSM-5 catalysts) on biomass weight loss at a heating rate of 20 °C/min and Ca/C ratio of 0.3. Previously, it was reported that the volatilization of the CaO and pine wood blends takes place between 200 and 700 °C [14]. In Fig. 8(a), the TG curve shows similar weight loss tendency when the temperature is no more than 400 °C (the dehydration stage and part of the volatilization stage). In comparison, the TG curve of catalytic pyrolysis appears different at the hightemperature of the volatilization stage and decomposition stage. Further, the pine wood sample degrades faster than the blends from 400 to 500 °C. With the temperature increasing up to 500 °C, the biomass conversion of pine wood using CaO/ZSM-5 and CaO catalysts (94.7% and 85.3%, respectively) exceeds the pine wood sample gradually. Specifically, the catalyst blends are 10.8% and 1.3% higher than that of pine wood sample at 950 °C. Fig. 8 (b) presents the pine wood conversion in terms of the conversion  $(\alpha)$  and the differential conversion  $(d\alpha/dT)$  as a function of temperature. Both profiles for biomass pyrolysis are generated at a heating rate of 20 °C/min and Ca/C ratio of 0.3. The figure indicates that under the same  $\alpha$  conditions from 0.7 to 0.9, the corresponding temperature shows difference between the catalysts blends and pure pine wood and follows the law: CaO/ZSM-5 > CaO > pine wood. It is explained that the released H<sub>2</sub>O or CO<sub>2</sub> from pine wood pyrolysis will be captured at this temperature range and thus slows down the weight decrease of the blended samples.

## 3.2.3. Effect of the Ca/C ratio

Fig. 9(a) presents TG curve for pine wood pyrolysis with CaO/ZSM-5 catalyst blends at different Ca/C ratios and a heating rate of 20 °C/min. The TG curve shows a much different trend at temperatures higher than 400 °C. Further, the effect of Ca/C ratio of CaO/ZSM-5 catalysts on weight loss becomes much more obvious at 700 °C. We also observe that the pine wood weight loss using CaO/ZSM-5 catalyst blends increases slightly in the temperature range 50–200 °C with an increasing Ca/C ratio. For temperatures higher than 600 °C, the pine wood conversion increase with increasing Ca/C ratio, which indicates that the addition of the CaO/ZSM-5 catalysts improves the conversion of biomass to syngas and bio-oils. Furthermore, increasing the Ca/C ratio enhances the pine wood conversion.

The effect of the Ca/C ratio (CaO/ZSM-5 catalyst) and heating rate on the maximum DTG distributions is shown in Fig. 9(b). A linear increase in maximum DTG can be observed with increasing heating rate. The maximum peak of DTG curves occurred mainly at 350–400 °C, which corresponds with the main weight loss of the TG curves. It can also be seen that the maximum DTG decreases slightly under the same heating rate with the Ca/C ratio increasing. It is believed that the hemicellulose, cellulose, and lignin of pine wood were lumped together to form the highest peak of DTG curves.  $CO_2$  is generated from decomposition of pine wood and captured by CaO or CaO/ZSM-5 catalyst. Thus, it can be concluded that the adsorption of the produced  $CO_2$  on CaO/ZSM-5 catalyst which reduces the weight loss rate.

# 3.3. Model-free kinetic analysis

The kinetic parameters such as activation energy and preexponential factor were obtained from the model-free nonisothermal TGA. WFO and KAS methods are adopted for kinetics analysis in this study. Fig. 10 presents (a) FWO plots of  $ln(\beta)$  versus -1/T of pine wood; (b) KAS plots of  $\ln(\beta/T^2)$  versus -1/T of pine wood; (c) FWO plots of pine wood with CaO/ZSM-5 catalyst blends at Ca/C ratio of 0.1; (d) KAS plots of pine wood with CaO/ZSM-5 catalyst blends at Ca/C ratio of 0.1; (e) FWO plots of pine wood with CaO/ZSM-5 catalyst blends at Ca/C ratio of 0.2; (f) KAS plots of pine wood with CaO/ZSM-5 catalyst blends at Ca/C ratio of 0.2; FWO plots of pine wood with CaO/ZSM-5 catalyst blends at Ca/C ratio of 0.3; (f) KAS plots of pine wood with CaO/ZSM-5 catalyst blends at Ca/C ratio of 0.3, respectively. The conversion ( $\alpha$ ) was calculated according to Eq. (2). To determine the kinetic parameters from FWO and KAS methods, the values of  $\alpha$  were chosen from 0.2 to 0.9 because significant experimental errors may occur at the lowest or largest  $\alpha$  values. As such, the activation energy can be calculated from the linear fit for each value of  $\alpha$  by using Eq. (9) and Eq. (10).

The activation energy values calculated at the heating rate of 10, 20, 30, and 40 °C/min with selected values of  $\alpha$  (from 0.2 to 0.9)

**Table 3**BET surface area and pore volume of ZSM-5 zeolite, CaO, and CaO/ZSM-5 catalyst.

Catalyst	BET surface area (m²/g)	Pore volume (cm³/g)
ZSM-5 zeolite	413.5	0.33
CaO	87.3	0.16
CaO/ZSM-5	204.0	0.62

**Table 4** The activation energy and  $R^2$  values at 10, 20, 30, and 40 °C/min by FWO and KAS methods using CaO/ZSM-5 catalyst.

Samples	α	FWO method		KAS method	
		E (kJ mol <sup>-1</sup> )	R <sup>2</sup>	E (kJ mol <sup>-1</sup> )	R <sup>2</sup>
Ca/C = 0	0.2	167.6	0.99900	149.6	0.99889
	0.3	172.1	0.99973	153.6	0.99970
	0.4	175.2	0.99990	156.3	0.99989
	0.5	177.5	0.99996	158.2	0.99996
	0.6	178.6	0.99995	159.1	0.99994
	0.7	179.1	0.99987	159.5	0.99984
	0.8	179.6	0.99964	159.8	0.99957
	0.9	208.9	0.96582	187.0	0.96140
	Average	179.8	-	160.4	-
Ca/C = 0.1	0.2	169.0	0.99991	150.9	0.99990
	0.3	172.5	0.99988	153.9	0.99987
	0.4	175.0	0.99983	156.0	0.99980
	0.5	176.1	0.99977	156.8	0.99974
	0.6	176.6	0.99982	157.2	0.99979
	0.7	177.3	0.99976	157.7	0.99972
	0.8	183.7	0.99619	163.5	0.99560
	0.9	228.0	0.94721	203.6	0.94027
	Average	182.3	-	162.4	=
Ca/C = 0.2	0.2	153.1	0.99410	133.8	0.99502
	0.3	160.8	0.99706	141.4	0.99722
	0.4	166.0	0.99824	146.6	0.99811
	0.5	170.7	0.99885	151.1	0.99863
	0.6	173.5	0.99900	154.2	0.99888
	0.7	174.2	0.99738	155.8	0.99784
	0.8	177.0	0.89862	151.1	0.86764
	0.9	215.5	0.88685	189.9	0.86964
	Average	173.8	-	153.0	-
Ca/C = 0.3	0.2	148.2	0.92158	131.0	0.90961
	0.3	158.0	0.96727	140.0	0.96219
	0.4	163.2	0.98698	144.7	0.98489
	0.5	166.5	0.99659	148.1	0.99600
	0.6	167.2	0.99974	138.5	0.99967
	0.7	157.4	0.99373	132.1	0.99275
	0.8	136.7	0.96851	117.5	0.96179
	0.9	179.8	0.96818	155.2	0.96124
	Average	159.6	-	138.4	-

using CaO/ZSM-5 catalyst are shown in Table 3. It is observed that: (1) the  $R^2$  of all the curves are within 0.92–1.00 (FWO method) and 0.91–1.00 (KAS method), except when the Ca/C ratio is 0.2 and  $\alpha$  at 0.8 and 0.9. This is a good quality of fit; (2) compared with non-catalytic pyrolysis, a significant temperature increase is required to achieve the same  $\alpha$  when using pine wood with CaO/ZSM-5 catalyst blends, as seen in Fig. 8(b). Thus, it can be observed that the  $R^2$  of the curves fitting is relatively low when  $\alpha$  is higher than 0.7; (3) the activation energy of pine wood with CaO/ZSM-5 catalyst blends increase with the increase in Ca/C ratio at an  $\alpha$  range from 0.2 to 0.9. Furthermore, when the biomass conversion increases from 0.8 to 0.9, the activation energy shows a significant increase due to the calcination of calcium carbonate Table 4.

The effects of heating rates and Ca/C ratios on the pine wood conversion distributions were investigated to determine better portioning condition for biomass pyrolysis. Fig. 11(a) and (b) present the biomass conversion distributions using CaO and CaO/ZSM-5 catalysts, respectively. For pine wood pyrolysis with CaO blends, the biomass conversion shows little differences at different heating rates and Ca/C ratios. The maximum and the minimum pine wood conversion occurs at the heating rate of 30 °C/min, Ca/C ratio at 0 and heating rate of 20 °C/min, Ca/C ratio at 0.2. As for pine wood pyrolysis with CaO/ZSM-5 catalyst blends, the conversion distributions show much obvious regularity. The results indicate that the heating rate shows little influence on the pine wood

conversion while the Ca/C ratio is a more important influencing factor. With the increasing of Ca/C ratio, the pine wood conversion increases by more than 11 %.

The activation energy distributions for different conversions and Ca/C ratios using CaO/ZSM-5 catalyst are examined in Fig. 11 (c) (FWO method), Fig. 11(d) (KAS method), respectively. It is found that within an  $\alpha$  value of 0.2–0.9 and Ca/C ratio from 0 to 0.3, the values of activation energy obey the following trends: (1) the activation energy is stable and shows relatively small difference at the left half of the area when  $\alpha$  is no more than 0.8; (2) a Ca/C ratio of 0.3 produces the minimum values of activation energy, which is probably due to the heat release by calcium oxide carbonation; (3) the maximum activation energy was found at the upper part of the area because the generated CaCO $_3$  decomposes into CaO and absorbs much energy.

#### 4. Conclusions

In this study, hierarchical porosity has been produced in the ZSM-5 zeolite by using alkali treatment. CaO was synthesized with the modified ZSM-5 zeolite to form the CaO/ZSM-5 catalyst. It has been shown that the CaO was dispersed in the skeleton structure of the ZSM-5 uniformly by SEM and EDS mapping. The pyrolysis characteristics and kinetic behavior of pine wood with catalysts blends

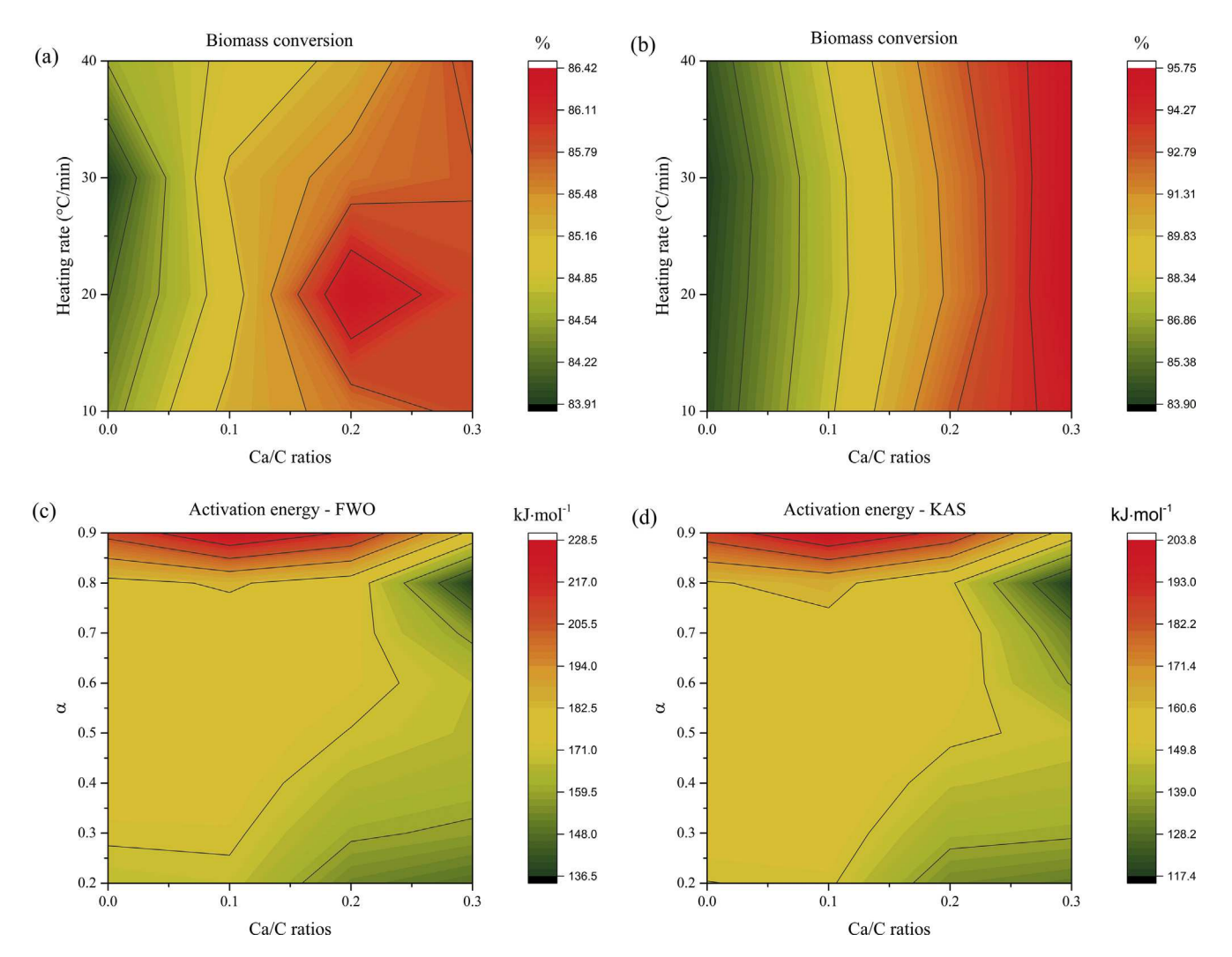


Fig. 11. Pine wood conversion distributions under different Ca/C ratios and heating rates by using (a): CaO; (b): CaO/ZSM-5 catalyst; and activation energy distributions under different conversion and Ca/C ratios by using: (c) FWO method; (d) KAS method.

(CaO and CaO/ZSM-5) were investigated at different Ca/C ratios (0, 0.1, 0.2 and 0.3) and different heating rates (10, 20, 30, and 40 °C/min). The effects of calcium content (Ca/C ratio), heating rates, and different kinds of catalysts on the pine wood conversion were also examined. The results show that the biomass conversion has been promoted by 0.8%, 2.2%, and 1.7% (Ca/C ratios at 0.1, 0.2, and 0.3) using CaO catalyst and 3.5%, 7.3%, and 11.5% using CaO/ZSM-5 catalyst (at the heating rate of 20 °C/min).

Thermogravimetric analysis was used to study the thermal decomposition behavior and kinetics of pine wood and pine wood catalytic pyrolysis over the CaO/ZSM-5 catalyst. The model-free FWO and KAS methods were used to estimate the kinetic parameters. The average activation energy obtained by FWO method is 179.8, 182.3, 173.8, and 159.6 kJ/mol; 160.4, 162.4, 153.0, and 138.4 kJ/mol by KAS method for Ca/C ratios at 0, 0.1, 0.2, and 0.3, respectively. The results imply that the addition of the CaO/ZSM-5 catalyst in the biomass pyrolysis process could appreciably promote pine wood conversion. Moreover, CaO/ZSM-5 catalyst shows a promising effect on activation energy and decreases the activation energy in a certain Ca/C ratio range.

#### Acknowledgements

This work was supported by the National Science Foundation [1632899] in the United States; Natural Science Foundation of China [51576042]; Natural Science Foundation of Jiangsu [BK20160672]Fundamental Research Funds for the Central Universities; the Foundation of Graduate Creative Program of Jiangsu [KYLX16-0200]; and the Scholarship Award for Excellent Doctoral Student granted to the first author by the Ministry of Education and China Scholarship Council.

#### References

- Lu KM, Lee WJ, Chen WH, Lin TC. Thermogravimetric analysis and kinetics of co-pyrolysis of raw/torrefied wood and coal blends. Appl Energy 2013:105:57-65.
- [2] Masnadi MS, Grace JR, Bi XT, Lim CJ, Ellis N. From fossil fuels towards renewables: Inhibitory and catalytic effects on carbon thermochemical conversion during co-gasification of biomass with fossil fuels. Appl Energy 2015;140:196–209.
- [3] Gradisher L, Dutcher B, Fan M. Catalytic hydrogen production from fossil fuels via the water gas shift reaction. Appl Energy 2015;139:335–49.
- [4] Ragauskas AJ, Williams CK, Davison BH, Britovsek G, Cairney J, Eckert CA, et al. The path forward for biofuels and biomaterials. Science 2006;311:484–9.
- [5] Park DK, Kim SD, Lee SH, Lee JG. Co-pyrolysis characteristics of sawdust and coal blend in TGA and a fixed bed reactor. Bioresour Technol 2010;101:6151-6.
- [6] Chen CX, Ma XQ. Liu K. Thermogravimetric analysis of microalgae combustion under different oxygen supply concentrations. Appl Energy 2011;88:3189–96.
- [7] Chen TJ, Zhang JZ, Wu JH. Kinetic and energy production analysis of pyrolysis of lignocellulosic biomass using a three-parallel Gaussian reaction model. Bioresour Technol 2016;211:502–8.
- [8] Lopez-Gonzalez D, Fernandez-Lopez M, Valverde JL, Sanchez-Silva L. Kinetic analysis and thermal characterization of the microalgae combustion process by thermal analysis coupled to mass spectrometry. Appl Energy 2014;114:227–37.
- [9] Maurya R, Ghosh T, Saravaia H, Paliwal C, Ghosh A, Mishra S. Non-isothermal pyrolysis of de-oiled microalgal biomass: kinetics and evolved gas analysis. Bioresour Technol 2016;221:251–61.
- [10] Ferrara F, Orsini A, Plaisant A, Pettinau A. Pyrolysis of coal, biomass and their blends: performance assessment by thermogravimetric analysis. Bioresour Technol 2014;171:433–41.
- [11] Zhang XS, Lei HW, Zhu L, Zhu XL, Qian M, Yadavalli G, et al. Thermal behavior and kinetic study for catalytic co-pyrolysis of biomass with plastics. Bioresour Technol 2016;220:233–8.
- [12] Foster AJ, Jae J, Cheng YT, Huber GW, Lobo RF. Optimizing the aromatic yield and distribution from catalytic fast pyrolysis of biomass over ZSM-5. Appl Catal A Gen 2012;423:154–61.
- [13] Gayubo AG, Aguayo AT, Atutxa A, Aguado R, Olazar M, Bilbao J. Transformation of oxygenate components of biomass pyrolysis oil on a HZSM-5 zeolite. II. Aldehydes, ketones, and acids. Ind Eng Chem Res 2004;43:2619–26.
- [14] Mabuda Al, Mamphweli NS, Meyer EL. Model free kinetic analysis of biomass/sorbent blends for gasification purposes. Renew Sust Energy Rev 2016;53:1656-64.

- [15] Lin XN, Zhang ZJ, Sun JP, Guo WJ, Wang QW. Effects of phosphorus-modified HZSM-5 on distribution of hydrocarbon compounds from wood-plastic composite pyrolysis using Py-GC/MS. J Anal Appl Pyrol 2015;116:223–30.
- [16] Jae J, Tompsett GA, Foster AJ, Hammond KD, Auerbach SM, Lobo RF, et al. Investigation into the shape selectivity of zeolite catalysts for biomass conversion. J Catal 2011;279:257–68.
- [17] Perez-Ramirez J, Christensen CH, Egeblad K, Christensen CH, Groen JC. Hierarchical zeolites: enhanced utilisation of microporous crystals in catalysis by advances in materials design. Chem Soc Rev 2008;37:2530–42.
- [18] Serrano DP, Escola JM, Pizarro P. Synthesis strategies in the search for hierarchical zeolites. Chem Soc Rev 2013;42:4004–35.
- [19] Chal R, Gerardin C, Bulut M, van Donk S. Overview and industrial assessment of synthesis strategies towards zeolites with mesoporous. Chem Cat Chem 2011;3:67–81.
- [20] Ahn JH, Kolvenbach R, Neudeck C, Al-Khattaf SS, Jentys A, Lercher JA. Tailoring mesoscopically structured H-ZSM5 zeolites for toluene methylation. J Catal 2014;311:271–80.
- [21] Li Y, Liu S, Xie S, et al. Promoted metal utilization capacity of alkali-treated zeolite: preparation of Zn/ZSM-5 and its application in 1-hexene aromatization. Appl Catal A Gen 2009;360:8–16.
- [22] Groen JC, Zhu W, Brouwer S, et al. Direct demonstration of enhanced diffusion in mesoporous ZSM-5 zeolite obtained via controlled desilication. J Am Chem Soc 2007;129:355–60.
- [23] Deng Q, Zhang XW, Wang L, Zou JJ. Catalytic isomerization and oligomerization of endo-dicyclopentadiene using alkali-treated hierarchical porous HZSM-5. Chem Eng Sci 2015;135:540-6.
- [24] Lu Q, Zhang ZF, Dong CQ, Zhu XF. Catalytic upgrading of biomass fast pyrolysis vapors with nano metal oxides: an analytical Py-GC/MS study. Energies 2010;11:1805–20.
- [25] Veses A, Aznar M, Martinez I, Martinez JD, Lopez JM, Navarro MV, et al. Catalytic pyrolysis of wood biomass in an auger reactor using calcium-based catalysts. Bioresour Technol 2014;162:250–8.
- [26] Liu SY, Xie QL, Zhang B, Cheng YL, Liu YH, Chen P, et al. Fast microwaveassisted catalytic co-pyrolysis of corn stover and scum for bio-oil production with CaO and HZSM-5 as the catalyst. Bioresour Technol 2016;204:164–70.
- [27] Sun LZ, Zhang XD, Chen L, Xie XP, Yang SX, Zhao BF, et al. Effect of preparation method on structure characteristics and fast pyrolysis of biomass with Fe/CaO catalysts. J Anal Appl Pyrol 2015;116:183–9.
- [28] Zhang XD, Sun LZ, Chen L, Xie XP, Zhao BF, Si HY, et al. Comparison of catalytic upgrading of biomass fast pyrolysis vapors over CaO and Fe(III)/CaO catalysts. J Anal Appl Pyrol 2014;108:35–40.
- [29] Yuan T, Tahmasebi A, Yu JL. Comparative study on pyrolysis of lignocellulosic and algal biomass using a thermogravimetric and a fixed-bed reactor. Bioresour Technol 2015;175:333–41.
- [30] Kandelbauer A, Wuzella G, Mahendran A, Taudes I, Widsten P. Model-free kinetic analysis of melamine-formaldehyde resin cure. Chem Eng J 2009;152:556-65.
- [31] Rizzo AM, Prussi M, Bettucci L, Libelli IM, Chiaramonti D. Characterization of microalga Chlorella as a fuel and its thermogravimetric behavior. Appl Energy 2013;102:24–31.
- [32] Slopiecka K, Bartocci P, Fantozzi F. Thermogravimetric analysis and kinetic study of poplar wood pyrolysis. Appl Energy 2012;97:491-7.
- [33] Huang YF, Chiueh PT, Kuan WH, Lo SL. Appl Energy 2013;110:1–8.
- [34] Zhou L, Zou H, Wang Y. Effect of potassium on thermogravimetric behavior and co-pyrolytic kinetics of wood biomass and low density polyethylene. Renew Energy 2017;102:34–141.
- [35] Williams PT, Nugranad N. Comparison of products from the pyrolysis and catalytic pyrolysis of rice husks. Energy 2000;25:493–513.
- [36] Wang X, Hu M, Hu WY, Chen ZH, Liu SM, Hu ZQ, et al. Thermogravimetric kinetic study of agricultural residue biomass pyrolysis based on combined kinetics. Bioresour Technol 2016;219:510–20.
- [37] Hu M, Chen ZH, Wang SK, Guo DB, Ma CF, Zhou Y, et al. Thermogravimetric kinetics of lignocellulosic biomass slow pyrolysis using distributed activation energy model, Fraser-Suzuki deconvolution, and iso-conversional method. Energy Convers Manage 2016;118:1–11.
- [38] Agrawal A, Chakraborty S. A kinetic study of pyrolysis and combustion of microalgae Chlorella vulgaris using thermo-gravimetric analysis. Bioresour Technol 2013;128:72–80.
- [39] Bartocci P, Anca-Couce A, Slopiecka K, et al. Pyrolysis of pellets made with biomass and glycerol: kinetic analysis and evolved gas analysis. Biomass Bioenergy 2017;97:11–9.
- [40] Chen CX, Ma XQ. He Y. Co-pyrolysis characteristics of microalgae Chlorella vulgaris and coal through TGA. Bioresour Technol 2012;117:264–73.
- [41] Sun Z, Xu CC, Chen SY, Xiang WG. Improvements of CaO-based sorbents for cyclic CO<sub>2</sub> capture using a wet mixing process. Chem Eng J 2016;286: 320–8.
- [42] Sun Z, Xiang WG, Chen SY. Sorption enhanced coal gasification for hydrogen production using a synthesized CaO-MgO-molecular sieve sorbent. Int J Hydrogen Energy 2016;41:17323–33.
- [43] Tang MC, Xu L, Fan MH. Effect of Ce on 5 wt% Ni/ZSM-5 catalysts in the CO<sub>2</sub> reforming of CH<sub>4</sub> reaction. Int J Hydrogen Energy 2014;39:15482–96.
- [44] Wang GW, Zhang JL, Shao JG, Liu ZJ, Zhang GH, Xu T, et al. Thermal behavior and kinetic analysis of co-combustion of waste biomass/low rank coal blends. Energy Convers Manage 2016;124:414–26.
- [45] Toscano G, Pizzi A, Pedretti EF, Rossini G, Ciceri G, Martignon G, et al. Torrefaction of tomato industry residues. Fuel 2015;143:89–97.

- [46] Okolo GN, Neomagus HWJP, Everson RC, Roberts MJ, Bunt JR, Sakurovs R, et al. Chemical-structural properties of South African bituminous coals: insights from wide angle XRD-carbon fraction analysis, ATR-FTIR, solid state 13 C NMR, and HRTEM techniques. Fuel 2015;158:779–92.
- [47] Rousset P, Aguiar C, Labbe N, Commandre JM. Enhancing the combustible properties of bamboo by torrefaction. Bioresour Technol 2011;102:8225–31.
   [48] Grzybek T, Maiti GC, Scholz D, Baerns M. Surface composition and selectivity of
- [48] Grzybek T, Maiti GC, Scholz D, Baerns M. Surface composition and selectivity of sodium-compound-impregnated calcium oxide catalysts for the oxidative coupling of methane. Appl Catal A Gen 1993;107:115–24.
- [49] Park YH, Kim J, Kim SS, Park YK. Pyrolysis characteristics and kinetics of oak trees using thermogravimetric analyzer and micro-tubing reactor. Bioresour Technol 2009;100:400–5.
- [50] Kalogiannis KG, Stefanidis SD, Michailof CM, et al. Pyrolysis of lignin with 2DGC quantification of lignin oil: effect of lignin type, process temperature and ZSM-5 in situ upgrading. J Anal Appl Pyrol 2015;115:410–8.